ENGINEERING TRANSACTIONS • *Engng. Trans.* • **64**, 3, 301–309, 2016
Polish Academy of Sciences • Institute of Fundamental Technological Research (IPPT PAN)
National Engineering School of Metz (ENIM) • Poznan University of Technology

The Effect of Process Parameters on Residual Stress in a Friction Stir Processed Cast Aluminium Alloy AlSi9Mg

Marek Stanisław WĘGLOWSKI[1)], Piotr SĘDEK[1)], Carter HAMILTON[2)]

[1)] *Institute of Welding*
Błogosławionego Czesława 16–18, 44-100 Gliwice
e-mail: marek.weglowski@is.gliwice.pl

[2)] *Department of Mechanical and Manufacturing Engineering*
Miami University, College of Engineering and Computing
Oxford, Ohio, USA

The effect of friction stir processing (FSP) on residual stress in a modified cast aluminium alloy AlSi9Mg is presented. The influence of rotational speed and tool type were analysed. The trepanation method was utilized to experimentally measure the residual stress. The results indicate that an increase in rotational speed causes an increase in residual stress. The region around the FSP bead was characterised by tensile residual stress fields which were balanced by compressive stresses in the parent material. A higher residual stress was observed on the advancing side than on the retreating side. Moreover, this asymmetry in residual stress distribution is due to the asymmetry in the volume of material plasticized along the advancing and retreating sides of the stir zone, generating the observed heat distribution. A higher level of residual stress was achieved with the Triflute tool than with a conventional tool.

Key words: cast aluminium alloy AlSi9Mg, friction stir processing, residual stress.

1. Introduction

Many different technologies can be used to refine the microstructure of aluminium alloys, such as squeeze casting [1], vibration [2], and electromagnetic stirring [3]. However, from a practical point of view, one of the most promising techniques is friction stir processing (FSP) [4–6]. FSP is a solid-state process in which a rotating cylindrical tool, essentially consisting of a pin and a shoulder (sometimes without a pin), is plunged into the modified material after which the tool then travels in the desired direction. The rotating shoulder generates heat which softens the material (below the melting temperature of the material) and with the mechanical stirring caused by the pin, the material within the processed zone undergoes intense plastic deformation yielding a dynamically recrystallised fine grain microstructure [7]. Previous investigations by this research team into

the field of FSP focused on the microstructure of cast aluminium alloys [4–6] and analysis of the process [8–9].

It should be noted that significant amounts of residual stresses can be generated during friction stir processing of cast aluminium alloys and can result in significant degradation of the structural integrity and performance of components. The measurement of residual stress in welding technologies can be accomplished through several methods: hole drilling [10], trepanation [11], ultrasonic [12], contour [l3], cut compliance [14], and neutron diffraction [15]. Previous results [15] have revealed that the measured residual stress profiles show relatively small through-thickness residual stress variations in a plate processed with both a stirring pin and tool shoulder, while there are significant through-thickness residual stress variations in a plate processed only with the tool shoulder. Residual stresses were measured through the thickness of FSP 6061-T6 aluminium-alloy plates using neutron diffraction. The authors [16] revealed that the residual stress profiles indicated a mild asymmetry within the welds with the stresses being about 10% higher on the advancing (shear) side. They also indicated that an increase in the travelling speed causes an increase in the residual stress.

The goal of this paper is to understand the relationship between FSP parameters and residual stress distribution. The results will be useful for the development of more accurate numerical simulations.

2. Work methodology

FSP samples were fabricated using as-cast AlSi9Mg plates. Plates approximately 306 mm long, 306 mm wide, and 6.0 mm thick were used in the experiment (Fig. 1). Samples were made at three different tool rotational speeds: 560, 710 and 900 revolutions per minute (rpm), and one traveling speed: 560 mm/min. Two different kinds of tool were used: a conventional cylindrical threaded pin

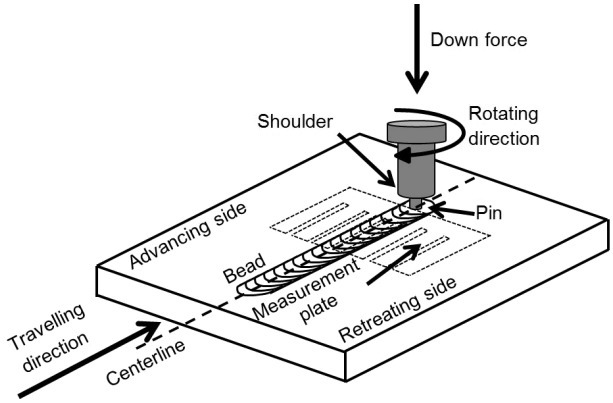

Fig. 1. Schematic of FSP and measurement plate of residual stress position.

and a Triflute pin (Fig. 2). The tools had a shoulder diameter of 22 mm, pin diameter of 8 mm, and pin depth of 4.5 mm. The tools were made from HS6-5-2 high speed steel.

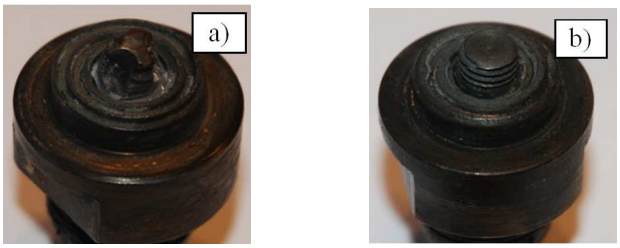

FIG. 2. FSP tool used during experiments: a) Triflute tool, b) conventional tool.

The FSP machine was equipped with an appropriate device for measuring torque and forces (down force and travelling force). The mean value of the spindle torque was measured by the LOWSTIR head and calculated from 1000 points in the area of the fully stabilised FSP process.

The trepanation method was utilized to experimentally measure the residual stress. In this method, the difference in length between reference points before and after the release of stress correlates to the residual stress component along the measurement axis. The longitudinal welding stresses, therefore, are computed using the following formula:

$$\sigma_W = \frac{\Delta L}{L} E \tag{2.1}$$

where E – longitudinal modulus of elasticity [N/mm^2], ΔL – difference between the reference length on the tested piece and the reference length on the standard block [mm·10^{-4}], L – initial reference length on the workpiece [mm].

A detailed description of this method was presented in a previous paper by the authors [17]. A view of the measurement plate for the trepanation method with incisions to release internal stresses is shown in Fig. 3. Macrostructural examination was conducted with light microscopy (LM, NIKON MA200).

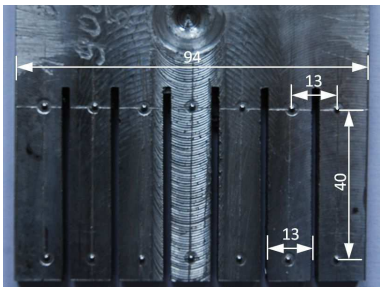

FIG. 3. View of measurement plate for trepanation method with incisions to release internal stresses.

3. Results and discussion

The influence of rotation speed on the longitudinal residual stress profiles for a conventional tool is presented in Fig. 4 and for a Triflute tool in Fig. 5. The profiles have a characteristic peak-and-valley and asymmetric shape. In all cases, low tensile residual stresses occur in the centre of the stir zone. After rising at the advancing and retreating sides, the residual stresses fall and become compressive at 10–15 mm from the weld centreline. This profile shape has been observed previously in 5xxx series aluminium friction stir welds [16].

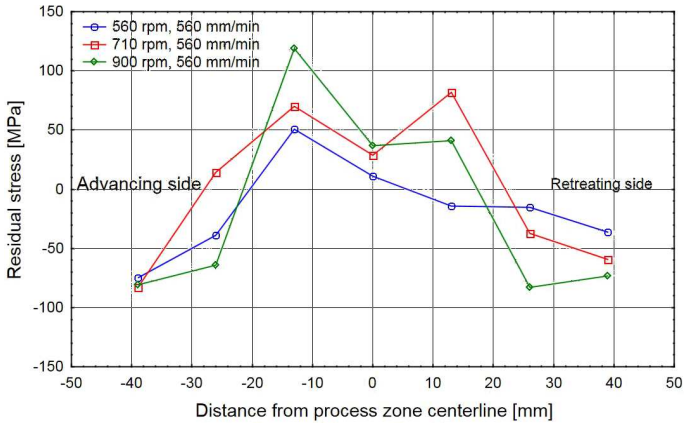

Fig. 4. Influence of rotation speed on residual stress profile, conventional tool.

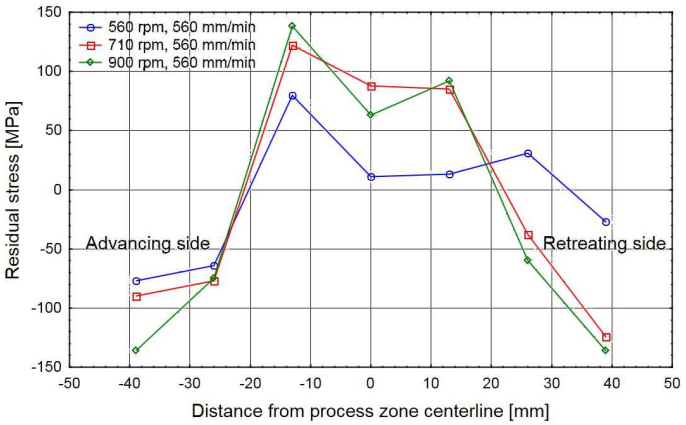

Fig. 5. Influence of rotation speed on residual stress profile, Triflute tool.

Aluminium has a high thermal conductivity, and this allows the heat generated by the friction of the tool to spread over a wide range. Furthermore, the coefficient of thermal dilation is high, and, combined with a relatively low yield

stress and an extremely rigid gripping system, residual stresses are generated while the processing bead is cooling. The FSP bead and the thermally altered area cool after the modification process, but their contraction to the original positions is prevented by the extremely rigid grips and the colder and unaffected aluminium that surrounds them. These elements generate transverse and longitudinal residual stresses.

The distribution of the asymmetric residual stresses in the workpiece is caused by an asymmetric temperature distribution [18, 19] as well as material flow in the stir zone. The material flows from the retreating side, across the FSP bead centreline to the advancing side. The tool is tilted from a vertical position to increase the forging action. To provide a stable process, the presence of a backing plate and side clamping forces is essential. The advancing side is the side of the FSP bead where the rotation of the tool and the forward motion are in the same direction, and the retreating side is the side where the rotation and the forward motion are opposite. The advancing side of the weld is normally the hotter side of the weld zone because the material flows from the retreating side, across the FSP bead centre line to the advancing side.

It should be noted that an increase in rotation speed causes an increase in the temperature within the stir zone [8, 20] as well as a decrease in the volume of modified (mechanically mixed) material caused by the shoulder [6]. For a given travelling speed, a higher tool rotation speed corresponds to a higher energy input per unit length of bead. The parameters recorded during FSP process are given in Table 1.

Table 1. Parameters recorded during FSP process.

No	Tool	ω [rpm]	Parameters		
			M [N · m]	F_d [kN]	F_v [kN]
1	Conventional	560	56.05	19.61	1.46
2		710	45.77	15.55	0.93
3		900	35.09	15.37	0.67
4	Triflute	560	51.79	16.37	1.34
5		710	44.19	18.78	1.13
6		900	34.49	19.88	1.69

Where M – spindle torque acting on the FSP tool, F_d – down force, F_v – force acting in the travelling direction.

Therefore, an increase in the rotational speed causes an increase in the temperature gradient, and thus increases distortion and stress levels. The same situation can be observed for both tools.

The Triflute tool is composed of three tapering, threaded re-entrant flutes that promote and amplify the material flow around the tool. The Triflute probe displaces substantially less material during modification than the conventional cylindrical pin type probe (see Fig. 6), and a lower spindle torque is acting on the tool (Table 1). Thus, with heat generated in a smaller volume of stir material, a higher gradient of temperature is observed. Therefore, higher stress levels in the modified material are observed. For the same rotational and travelling speed, the residual stress for the Triflute tool is much higher.

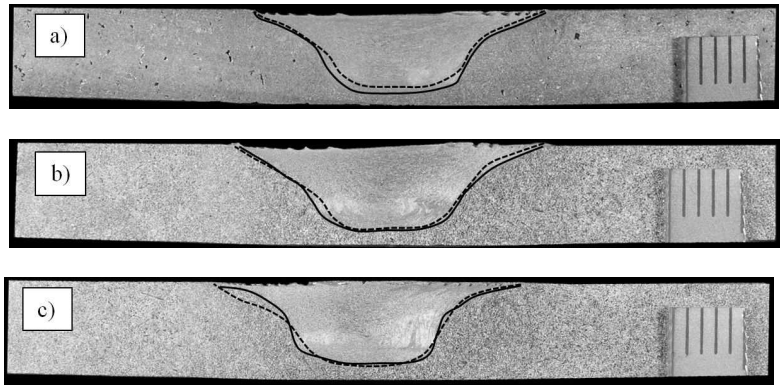

FIG. 6. Influence of tool on macrostructure of stir zone, a) 560 rpm, b) 710 rpm, c) 900 rpm; dash line is for Triflute tool, continuous line is for conventional tool.

The asymmetric distribution of residual stress is also directly linked with the difference in microstructure which can be observed for both the advancing and retreating sides. The macrostructure of the Al-Si alloy subjected to the FSP process is shown in Fig. 7.

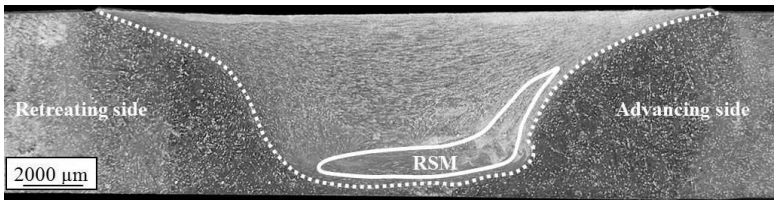

FIG. 7. Cross section of FSP area (advancing side on right side), light microscope.

The material flow during FSP is a complicated process and depends on the tool geometry, process parameters, and material. The threaded pins (conventional or Triflute) result in a superimposed vertical and horizontal material flow

from geometrical considerations. The threads tend to move material downward along the pin wall, and once this material reaches the bottom, the geometrical constraints require that the material moves up and away from the pin wall. The lateral traverse of the pin requires that the material moves from front to back. The "stirring" of material causes movement of the material from the retreating side around the pin to the advancing side. During each rotation of the tool, a semi-cylindrical portion of the material is pushed to the back of the tool and around to the retreating side.

The interaction among these three material flow patterns, based on geometrical and volume constraints, is complex. In the stir zone, as marked by the dotted curve, the shoulder flow zone (upper region) and pin stir zone (below) can be separated. As can be seen, the stir zone displays a region of rotational shear material – RSM (solid curve in Fig. 7) on the advancing side, extending but tailing off towards the retreating side in the mid-to-lower part of the zone. In the RSM region, Si particles have become quite evenly distributed in the α-Al matrix. The rest of the stir zone (outside the RSM region) is the material that has been deformed, but much less extensively, particularly towards the retreating sides (RS), and thus the Si particles originally concentrated in the interdendritic regions have remained, and the microstructure is still highly segregated. For the typical FSP parameters, $\omega = 560$ rpm, $v = 560$ mm/min, the RSM is quite low.

Shoulder driven and pin driven flows have been detected in the stir zones processed with these both tools, as illustrated in Fig. 8b, and the transition between stir zone and the thermomechanical affected zone (TMAZ) is more abrupt on the advancing side than on the retreating side, as observed in Figs. 8a and 8c. Material flow in the stir zone is difficult to evaluate because the microstructure is very refined and homogeneous (Fig. 8b) although an upward material flow is suggested by the deformation of the non-recrystallised grains on the advancing side (see Fig. 8c). Figure 8b shows that the transition between recrystallised and non-recrystallised regions is smoother on the retreating side.

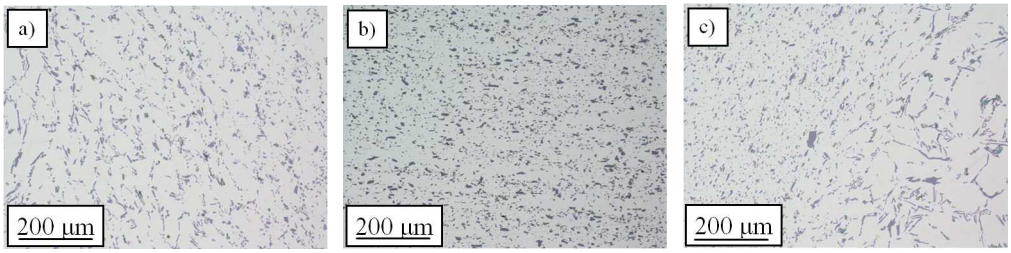

FIG. 8. Microstructural characteristics in the: a) retreating side, b) stir zone and c) advancing side.

4. Conclusions

The present study has examined the residual stresses caused by the FSP of a modified cast aluminium alloy AlSi9Mg. The results are as follows:

- The asymmetry in residual stress distribution is due to the asymmetry in the plasticised material volume along the advancing and retreating sides of the stir zone that generated the heat.
- An increase in rotational speed causes an increase in residual stress level, a higher stress level in the modified material can be observed for the Triflute tool than for the conventional tool.
- An increase in rotation speed causes a decrease in the spindle torque acting on the FSP tool.
- A lower spindle torque acting on the FSP tool is observed for the Triflute tool than for the conventional tool.

Acknowledgment

This work was performed with funding from Ministry of Science and Higher Education in Poland within the framework of statutory activity (Institute of Welding) and research grant No N507 295439 (AGH University of Science and Technology).

References

1. Ciućka T., *Influence of vibration during crystallization on mechanical properties and porosity of EN AC-AlSi17 Alloy*, Archives of Foundry Engineering, **13**(1): 5–18, 2013.
2. Zyska A., Konopka Z., Łągiewka M., Nadolski M., *Optimization of squeeze parameters and modification of AlSi7Mg alloy*, Archives of Foundry Engineering, **13**(2): 113–116, 2013.
3. Wrobel T., Szajnar J., *Modification of pure al and AlSi2 alloy primary structure with use of electromagnetic stirring method*, Archives of Metallurgy and Materials, **58**(3): 941–944, 2013.
4. Węglowski M.St., *Microstructure of cast aluminium alloy AlSi9Mg after FSP process*, Archives of Foundry Engineering, **14**(3): 75–78, 2014.
5. Węglowski M.St., Dymek S., *Friction stir processing of an AlSi6Cu4 cast aluminium alloy*, Archives of Foundry Engineering, **11**(2): 213–217, 2011.
6. Węglowski M.St., Dymek S., *Microstructural modification of cast aluminium alloy AlSi9Mg via friction modified processing*, Archives of Metallurgy and Materials, **57**(1): 71–78, 2012.
7. Darras B.M., Khraisheh M.K., *et al.*, *Friction stir processing of commercial AZ31 magnesium alloy*, Journal of Materials Processing Technology, **191**: 77–81, 2007.

8. Węglowski M.St., Pietras A., *Friction stir processing – analysis of the process*, Archives of Metallurgy and Materials, **56**: 779–788, 2011.

9. Węglowski M.St., Dymek S., Hamilton C., *Experimental investigation and modelling of friction stir processing of cast aluminium alloy AlSi9Mg*, Bulletin of the Polish Academy of Sciences – Technical Sciences, **61**: 893–904, 2013.

10. Węglowski M.St., Kwieciński K., Krasnowski K., Jachym R., *Characteristics of Nd: YAG laser welded joints of dual phase steel*, Archives of Civil and Mechanical Engineering, **9**(4): 85–97, 2009.

11. Hamilton C., Węglowski M.St., Dymek S., Sedek P., *Using a coupled thermal/material flow model to predict residual stress in friction stir processed AlMg9Si*, Journal of Materials Engineering and Performance, **24**: 1305–1312, 2015.

12. Sadeghi S., Najafabadi M.A., *et al.*, *Using ultrasonic waves and finite element method to evaluate through-thickness residual stresses distribution in the friction stir welding of aluminium plates*, Materials & Design, **52**: 870–880, 2013.

13. Liu Ch., Yi X., *Residual stress measurement on AA6061-T6 aluminium alloy friction stir butt welds using contour method*, Materials and Design, **46**: 366–371, 2013.

14. Ghidini T., Vugrin T., Dalle Donne C., *Residual stresses, defects and non-destructive evaluation of FSW joints*, Welding International, **19**(10): 783–790, 2005.

15. Woo W., Choo H., Brown D.W., Feng Z., Liaw P.K., *Angular distortion and through-thickness residual stress distribution in the friction-stir processed 6061-T6 aluminium alloy*, Materials Science and Engineering A, **437(**1): 64–69, 2006.

16. Peel M., Steuwer A., Preuss M., Withers P.J., *Microstructure, mechanical properties and residual stresses as a function of welding speed in aluminium AA5083 friction stir welds*, Acta Materialia, **51**(16): 4791–4801, 2003.

17. Węglowski M.St., Sedek P., Hamilton C., *Experimental and numerical analysis of residual stress in cast aluminium alloy after FSP process*, Key Engineering Materials, **682**: 18–23, 2016.

18. Hamilton C., Kopyściański M., Senkov O., Dymek S., *A coupled thermal/material flow model of friction stir welding applied to Sc-modified aluminium alloys*, Metallurgical and Materials Transactions A, **44**: 1730–1740, 2013.

19. Kishta E.E.M., Abed F.H., Darras B.M., *Nonlinear finite element simulation of friction stir processing of marine grade 5083 aluminium alloy*, Engineering Transactions, **62**(4): 313–328, 2014.

20. Hamilton C., Sommers A., Dymek S., *A thermal model of friction stir welding applied to Sc-modified Al-Zn-Mg-Cu alloy extrusions*, International Journal of Machine Tools & Manufacture, **49**: 230–238, 2009.

Received April 6, 2015; accepted version May 11, 2016.